HHS Public Access

Author manuscript

Int J Pharm. Author manuscript; available in PMC 2021 January 25.

Published in final edited form as:

Int J Pharm. 2020 January 25; 574: 118871. doi:10.1016/j.ijpharm.2019.118871.

A method to rapidly analyze the simultaneous release of multiple pharmaceuticals from electrospun fibers

Nicholas J. Schaub[a,b,c,*], **Joseph M. Corey**[a,b,d]

[a]Department of Neurology, University of Michigan, Ann Arbor, Michigan, United States

[b]Geriatrics Research, Education, and Clinical Center, Veterans Administration Ann Arbor Healthcare Center, Ann Arbor, Michigan, United States

[c]National Center for the Advancement of Translational Sciences, National Institutes of Health, Rockville, Maryland, United States

[d]Department of Biomedical Engineering, University of Michigan,Ann Arbor, Michigan, United States

Abstract

Electrospun fibers are a commonly used cell scaffold and have also been used as pharmaceutical delivery devices. In this study, we developed a method to analyze the release of multiple pharmaceuticals from a single electrospun fiber scaffold and determine how each pharmaceutical's loading concentration affects the release rate of each pharmaceutical. Our analysis methods were tested on electrospun fibers loaded with two pharmaceuticals: 6-aminonicotinamide (6AN) and ibuprofen. Pharmaceutical concentration in electrospun fibers ranged from 1.5% to 8.5% by weight. We found that 6AN release was dependent on the concentration of 6AN and ibuprofen loaded into the fibers, while ibuprofen release was only dependent on the loading concentration of ibuprofen but not 6AN. Unexpectedly, ibuprofen release became dependent on both 6AN and ibuprofen loading concentrations when fibers were aged for 1-month post-fabrication at room temperature in the laboratory followed by a 4-hour incubation inside the cell culture incubator at 37 °C and 5% CO_2. One additional discovery was an unknown signal that was attributed to the medical grade syringes used for electrospinning, which was easily removed using our method. These results demonstrate the utility of the methods developed here and indicate multiple agents can be released concomitantly from electrospun fibers to meet the demands of more complex tissue engineering approaches. Future work will focus on analysis of pharmaceutical release profiles to exploit the dependencies on pharmaceutical loading concentrations.

[*]Corresponding author at: National Center for the Advancement of Translational Science, 9800 Medical Center Drive, Rockville, MD 20850, United States. Nick.Schaub@nih.gov (N.J. Schaub).

6. Disclosure

No potential conflict of interest was reported by the authors.

Declaration of Competing Interest

The authors declare that they have no known competing financial interests or personal relationships that could have appeared to influence the work reported in this paper.

Appendix A. Supplementary material

Supplementary data to this article can be found online at https://doi.org/10.1016/j.ijpharm.2019.118871.

Keywords

6-Aminonicotinamide; Ibuprofen; Electrospun fibers; Pharmaceutical delivery; Drug-delivery

1. Introduction

Tissue engineering has become increasingly complex. State of the art approaches to regenerating tissue (such as the spinal cord) use a cocktail of bioactive agents in combination with a cellular scaffold (Silver and Miller, 2004; Cregg et al., 2014). There is a need to develop pharmaceutical delivery devices that meet the demands of these complicated approaches. Electrospun fibers are a common type of synthetic biomaterial used in tissue engineering as both a cellular scaffold (Schaub et al., 2015; Schaub, n.d.; Venugopal et al., 2008; Liao et al., 2006; Wang et al., 2013; Jiang et al., 2010; Pham et al., 2006; Holzwarth and Ma, 2011; Cao et al., 2009) and a means of delivering bioactive agents (Hu et al., 2014; Chou et al., 2015; Jang et al., 2009; Sill and von Recum, 2008; Ji et al., 2011; Szentivanyi et al., 2011; Chakraborty et al., 2009; Hadjiargyrou and Chiu, 2008). Electrospun fibers are polymeric fibers with diameters on the nano- to micro scale; as such, they are biomimetic, resembling the geometric structure of fibrillary proteins in the extracellular matrix. Most of the literature on pharmaceutical delivery from electrospun fibers has focused on delivery of a single agent, but a few studies have reported the release of multiple agents using layered or mixed fiber mats where each fiber in a scaffold contains a single pharmaceutical (Thakur et al., 2008; Sundararaj et al., 2013). At least one study has released multiple pharmaceuticals from a single fiber mat (Thakur et al., 2008), but no study has investigated how multi-pharmaceutical release is affected by changing each pharmaceuticals initial loading. Understanding how multiple pharmaceuticals are released from a single scaffold may permit new approaches to engineering pharmaceutical delivery devices that meet the demand for the increasing complexity of the tissue engineering field.

Pharmaceutical diffusion from a polymer depends on a variety of factors, including pharmaceutical/polymer affinity, pharmaceutical hydrophobicity, and concentration ratio of pharmaceutical to polymer (Chou et al., 2015; Zeng et al., 2005; Zeng et al., 2003). When multiple pharmaceuticals are added to fibers, additional factors, such as pharmaceutical/pharmaceutical affinity and the relative strength of each pharmaceutical's affinity for the polymer, need to be considered. An analysis of how pharmaceuticals interact with each other and the polymer may provide insight into new approaches to engineering release by taking advantage of these interactions. In this study, we develop an approach to studying how loading concentrations of multiple pharmaceuticals affect the release rate of each individual pharmaceutical. To accomplish this, we use a central composite circumscribed (CCC) experimental design. This experimental design is commonly used in engineering to identify trends in a process when multiple factors are involved, and we use it here to understand how each pharmaceutical's loading concentration influence the release of each pharmaceutical. Analysis of this experimental space should provide insight into how the release of each pharmaceutical is altered by its own loading concentration and the loading concentration of other pharmaceuticals.

In this study, we focused on the diffusion of small molecules from slowly degrading electrospun fibers. Because of the inherently slow growth and/or long distances required for some cells to grow (e.g. nerve regeneration), some tissue engineering applications require the use of slowly degrading scaffolds. Our laboratory has studied the use of aligned electrospun fibers as neurite guidance scaffolds (Corey et al., 2007; Corey et al., 2008; Gertz et al., 2010), and many other laboratories have also used electrospun fibers to guide neurite extension *in vitro* (Schaub et al., 2015; Koh et al., 2008; Yang et al., 2004; Wang et al., 2009; Wang et al., 2010; Alvarez-Perez et al., 2010; Prabhakaran et al., 2008) and *in vivo* (Hurtado et al., 2011; Liu et al., 2012; Chew et al., 2007; Neal et al., 2012; Gelain et al., 2011; Kim et al., 2008). The slow rate of nerve growth (~1 mm/day or less) (Pfister et al., 2011; Lundborg, 2003) will require slowly degrading materials to provide continuous physical cues throughout the duration of regeneration. For slowly degrading polymers, the dominant release mechanism is diffusion, and small molecules are more capable of diffusing out of a polymer compared to larger molecules (e.g. proteins). Further, small molecules have been released from slowly degrading electrospun poly-L-lactic acid (PLLA) fibers for up to two weeks (Schaub and Gilbert, 2011), and post fabrication processing allows release up to 45 days (D'Amato et al., 2017). A better understanding of pharmaceutical diffusion from slowly degrading fibers could aid in extending the duration of release of pharmaceuticals from electrospun fibers while maintaining fiber integrity over long time frames.

For this study, we used two small molecules (6AN and ibuprofen) that have (i) been released from electrospun fibers, (ii) have been used in neural tissue engineering, and (iii) have different release profiles. Ibuprofen is an anti-inflammatory agent that is also known to increase neurite extension through inhibition of Rho associated protein kinase (ROCK) (Fu et al., 2007; Roloff et al., 2015; Dill et al., 2010). Ibuprofen release is known to have a burst release profile from electrospun PLLA and PLGA (poly(lactic-co-glycolic) acid) fibers, where most of the pharmaceutical is released within in the first couple of days(Liu et al., 2017; Riggin et al., 2017). 6-Aminonicotinamide (6AN) is an anti-metabolite that targets the pentose phosphate shunt (Haghighat and McCandless, 1997) and is known to selectively target reactive astrocytes (Politis, 1989). 6AN is known to have an extended release profile (Schaub and Gilbert, 2011) that can be modified for extended release (greater than one month) with post-fabrication processing (D'Amato et al., 2017). The different release profiles of each pharmaceutical make them ideal candidates to study how the loading of multiple pharmaceuticals into electrospun fibers influences the release profile of each pharmaceuticals.

2. Methods

2.1. Materials & equipment

Electrospun fibers were generated using Poly-L-lactic acid (PLLA), 1,1,1,3,3,3-hexafluoro-2-propanol (HFP), 6-aminonicotinamide (6AN), and ibuprofen. PLLA with an inherent viscosity of 3.3 dl/g was purchased from Evonik (Resomer L210). HFP, 6AN, and ibuprofen were purchased from Sigma Aldrich. Relative humidity was monitored during electrospinning using an AM2302 relative humidity sensor (Digikey) attached to a Raspberry Pi (Newark Element 14) to record humidity levels throughout every

electrospinning trial. BD Syringes were purchased from VWR, and 23-gauge flat tip needles for electrospinning were purchased from Nordson EFD. Phosphate buffered saline (PBS) was purchased from Fisher Scientific. A Biotek Synergy HTX plate reader was used to acquire UV–Vis spectra of PBS exposed to drug loaded electrospun fibers. UV–Vis spectra were generated using UV transparent 96-well plates (Sigma Aldrich). Development of all algorithms and all data analysis was performed using MATLAB 2017b (Mathworks). Graphs were generated using Gramm (Morel, 2018).

2.2. UV–Vis spectral analysis of samples containing multiple drugs

2.2.1. Overview of method—We developed a method of identifying the concentrations of multiple drugs from a UV–Vis spectrum. Since the CCC design space grows exponentially with respect to the number of drugs released from the fibers, UV–Vis can provide a fast and accurate method of analyzing drug release relative to other methods of analyzing drug release (high performance liquid chromatography, liquid chromatography-mass spectrometry). The approach rigorously applies the Beer-Lambert law (Poggendorff, 1852; Lambert and Anding, 1892):

$$A(\lambda) = l \sum_{i=1}^{N} \varepsilon(\lambda)_i c_i \quad (1)$$

where $A(\lambda)$ is the absorption value at wavelength λ, l is the distance light traveled through the sample, $\varepsilon(\lambda)_i$ is the absorptivity of the i^{th} drug at wavelength λ, and c_i is the concentration of the i^{th} drug. We ignored l since the path length remained constant for this experiment. In this paper, $\varepsilon(\lambda)_i$ is the amount of absorbance per unit mass at the given wavelength.

This method involves two steps. The first step analyzes the UV–Vis spectrum of solutions with known quantities of drug to determine: i) the mass absorptivity, $\varepsilon(\lambda\varepsilon(\lambda)_i)_i$, ii) the upper concentration detection limit, iii) and lower concentration detection limit. The second step calculates the amount of drug in an unknown solution, where Eq. (1) is solved simultaneously at multiple wavelengths to determine each drug's concentration (c_ic_i). The solution to Eq. (1) in the drug detection step is the concentration of each drug that minimizes the error between the calculated absorbance from Eq. (1) and the actual absorbance in the UV–Vis spectrum.

2.2.2. Analysis of drug UV–Vis spectra—A two-fold serial dilution of each drug (6AN and Ibuprofen) was created in PBS. The maximum concentration was 500 μg/mL and the lowest was 0.488 μg/mL. 300 μL of each drug dilution was placed in a UV-transparent plate and a UV–Vis spectrum was generated (range = 200–500 nm, 1 nm step size). Control spectra were generated that contained only PBS (n = 4), and the replicates were averaged together and subtracted from the UV–Vis spectra of each drug. Examples of the background-corrected spectra for 6AN and Ibuprofen are shown in Fig. 1a and b respectively. The spectra from serial dilutions of 6AN and Ibuprofen are shown in Fig. 1c and d respectively.

After background subtraction, a linear regression was performed at each wavelength to determine the wavelength dependent mass absorptivity for each drug, $\varepsilon(\lambda\varepsilon(\lambda)_i)_i\varepsilon(\lambda)_i$, from

Eq. (1). Prior to performing the linear regression, absorbance values for drug dilutions were assessed to determine how many spectra had a detectable signal. We determined the lower limit of detection for the UV–Vis instrument to be 0.001 absorbance units (AU), which was about three standard deviations (SD = 0.00031 AU) larger than the signal between 400 nm and 500 nm of the PBS spectra. If all dilutions of a drug for a wavelength had an absorbance value less than 0.001, then the drug should not contribute any signal to a UV–Vis spectrum at that wavelength ($\varepsilon(\lambda\varepsilon(\lambda)_i)_i = 0\varepsilon(\lambda)_i = 0$) and no linear regression was performed. If one or two drug dilutions had an absorbance value greater than 0.001, then we discarded the wavelength from analysis since the drug may contribute to the signal but there is insufficient information to determine the mass absorptivity. If three or more wavelengths have absorbances values greater than 0.001 AU, then the following algorithm was used to determine the mass absorptivity, the upper concentration detection limit, and the lower concentration detection limit:

1. Perform a linear regression on all absorbance values with respect to concentration.
2. If the linear regression has (i) an $R^2 > 0.995$ or (ii) all residuals are less than 0.01 AU, then an optimal $\varepsilon(\lambda)_i$ has been found and no additional steps are required.
3. If a linear regression was performed on absorbance values from three concentrations and neither criteria from step 2 were met, then there is insufficient information to determine mass absorptivity. Absorbance values at this wavelength cannot be used to calculate drug concentration in unknown samples.
4. Perform two new linear regressions. First, perform a linear regression after removing the absorbance values from the largest concentration. Second, perform a second linear regression after removing the absorbance values from the smallest concentration.
5. If the R^2 value from the first linear regression is larger than the second linear regression, remove the largest concentration and absorbance values and go back to step 2. If the R^2 value from the second linear regression is larger than the first, remove the smallest concentration and absorbance values and go back to step 2.

Using this method, an $\varepsilon(\lambda\varepsilon(\lambda)_i)_i$ $\varepsilon(\lambda)_i$ was found for a range of concentrations. Fig. 1e-g show examples of linear fits for three different wavelengths. The slope of the solid line in Fig. 1e-g is the mass absorptivity for 6AN (orange) and ibuprofen (green), and the line indicates the points for which the mass absorptivity value fits the data with high accuracy. In addition to the mass absorptivity, the maximum and minimum detectable concentrations were recorded along with the absorbance value for the maximum and minimum detectable concentration. These values are used in the next step, where the amount of drug in solution is calculated using the values determined in the present step.

2.2.3. Calculation of unknown drug concentrations—Quantification of multiple drug concentrations in a sample involved finding a solution to Eq. (1) for all c_i that minimizes the error with respect to the UV–Vis spectrum of the sample. Although there is a linear relationship between absorbance and concentration, the mass absorbance, minimum

and maximum concentration detection limit is different for each wavelength. Ideally, Eq. (1) is solved for wavelengths where the unknown drug concentration falls between the minimum and maximum detection limits, while all other wavelengths are ignored. Since the drug concentration is not known, we used an iterative approach to solve Eq. (1). Each iteration updates the wavelengths selected to calculate each drug's concentration based on the predicted values of the previous iteration. This iterative process provides a solution after the error is below a threshold or ten iterations are completed.

The initial iteration uses the absorbance values of the unknown sample to determine which wavelengths are used to solve Eq. (1). The only wavelengths included in the initial calculation are wavelengths for which absorption values, $A(\lambda\varepsilon(\lambda)_i)A(\lambda)$, are greater than 0.001 and less than the maximum absorption values for all drugs (determined in 3.2.2). An initial calculation of drug concentrations, c_i, is made by minimizing the mean squared error:

$$\min_{c_i \in \mathbb{R}} \frac{1}{M} \sum_{\lambda=1}^{M} \left(A(\lambda) - \sum_{i=1}^{N} \varepsilon(\lambda)_i c_i \right)^2 \quad (2)$$

where $A(\lambda)$ is the absorbance value from the UV–Vis spectrum and $\sum_{i=1}^{N} \varepsilon(\lambda)_i c_i$ is the calculated absorbance based on calculated drug concentration. The initial drug concentration calculations were used to remove wavelengths from consideration for the next iteration. If the calculated concentrations were above or below the maximum or minimum detection limit respectively, the wavelength was ignored in the next iteration. If a drug had a negative predicted concentration, then the drug concentration was not predicted in subsequent iterations. Once a new set of wavelengths was selected, a new set of drug calculations were made according to Eq. (3) and the process was repeated until the mean squared error was less than 0.001 or ten iterations are completed.

2.2.4. Validation of drug detection method—The drug detection method described previously (Section 2.2.3) was validated with three different experiments. First, the UV–Vis spectra from serial dilutions of each drug were analyzed to determine if the detection algorithm could predict the amount of drug in each dilution. For each UV–Vis spectrum, the amounts of ibuprofen and 6AN were determined in each dilution. It was expected that only 6AN would be detected in the 6AN dilutions and only ibuprofen would be detected in the ibuprofen dilutions. Second, we mixed all combinations of the four lowest concentrations of each drug dilution together. The purpose of this experiment was to determine if we could correctly predict both drug concentrations in a sample containing known concentrations of both drugs. Third, we electrospun PLLA fibers containing only 6AN or only ibuprofen (electrospinning parameters are described in Section 2.3). In this experiment, it was expected that only 6AN or ibuprofen would be detected from each of the samples.

While analyzing UV–Vis spectra from drug released from electrospun fibers, we discovered an unknown signal in the spectra that we attributed to unknown chemicals that leached from the BD syringes (referred to as syringe components) used for electrospinning. To account for these unknown chemicals, a serial dilution of syringe components was created and analyzed using the method described in Section 2.2.2 to obtain mass absorptivity constants for every

wavelength. We isolated syringe components in syringes by placing 500 μL of a 70% ethanol solution into an electrospinning syringe. Parafilm was placed on the syringe tip to prevent evaporation. After seven days, the ethanol solution was removed from the syringe. Then, a two-fold serial dilution was performed using 70% ethanol. This procedure was repeated three times to determine repeatability. Since the identity of the syringe components and the quantity of chemical was unknown, the highest concentration of the ethanol solution was assigned a value of 500 μg/mL to mirror the concentrations used for the ibuprofen and 6AN serial dilutions.

2.3. Electrospinning

The electrospinning apparatus used in this study was previously described by Leach et al. (2011). Two groups of electrospun fibers were generated to validate the drug detection method described in Section 2.2. The first group (10% 6AN group) was electrospun fibers fabricated from a solution containing 10 mg of 6AN and 100.0 mg ± 0.5 mg of PLLA dissolved in 3.20 g ± 0.05 g of 1,1,1,3,3,3-hexafluor-2-propanol (HFP). The second group (10% ibuprofen group) was fabricated from the same solution as the 10% 6AN group, except 10 mg of Ibuprofen were dissolved into the solution instead of 10 mg of 6AN. Electrospun fibers were collected on 12 mm circular glass coverslips coated with a PLLA film. PLLA Films were deposited on glass coverslips by air casting a solution containing 100 mg of PLLA and 3 g of chloroform and 3 g of dichloromethane. Fibers were generated using a voltage of 12 kV, volumetric flow rate of 1.5 mL/hour, collected on a 25 cm diameter aluminum disk spinning at 1000 rpm, needle to collection disk distance of 6 cm, and a relative humidity of 23–28% was maintained throughout the electrospinning process. Fibers were collected for 10 min.

To evaluate how loading multiple drugs into electrospinning solutions affected drug release, we created fourteen electrospun scaffolds using a CCC experimental design (Table 1). The electrospinning solution for each sample used the same quantity of PLLA and HFP described in the previous paragraph but used different combinations of 6AN and Ibuprofen loading concentrations. Drug loading into the fibers is represented as a percentage of the weight of drug relative to the weight of polymer.

The center point of the CCC design was 5% 6AN and 5% Ibuprofen, which involved dissolving 5 mg each of 6AN and Ibuprofen into the electrospinning solution. Six solutions of 5% 6AN and 5% Ibuprofen were created. The other 8 samples were divided into two groups: linear effects samples and second order effects samples. The linear effects samples contained all combinations of 2.5% or 7.5% 6AN and 2.5% or 7.5% Ibuprofen. The second order effects samples contained 5% 6AN and 1.46% or 8.53% Ibuprofen, or 5% Ibuprofen and 1.46% or 8.53% 6AN. Only one replicate of the linear effects and second order effects samples were created since we want to model trends across groups rather than determine the reproducibility of the process. The drug loading concentrating values were chosen based on CCC experimental design, where the center point was 5% 6AN and 5% Ibuprofen, the linear effects groups had a 2.5% deviation from the center point (2.5% or 7.5% of each drug), and the second order effects had a deviation of $\sqrt{2}^{*}2.5\,\%$ create evenly spaced experimental data for the model in Eq. (3) that can be represented by a square for the linear components (Fig.

3a, purple square) and a circle for the second order effects (Fig. 3a, green circle) that circumscribe the square.

2.4. Evaluation of drug release from electrospun fiber scaffolds

2.4.1. Recording drug release from electrospun fibers—The day electrospun fiber samples were created, fiber samples were placed in a 24-well plate, submerged in 500 μL of PBS, and placed in a cell culture incubator (temperature 37° C, 5% CO_2). After two days, 300 μL of PBS from each sample was removed and analyzed by UV–Vis. Any remaining volume more than 300 μL was removed and measured with a pipettor by adjusting the volume setting on the pipettor such that all PBS was removed from the well without any air bubbles present in the pipette tip. The excess volume was recorded to determine the volume of PBS in the well after evaporation over the two-day incubation period. Fresh PBS was then placed onto each electrospun fiber sample and placed back into the incubator. Each UV–Vis spectrum was analyzed using the method described in Section 2.2.3 to determine the amount of ibuprofen and 6AN released into PBS exposed to the fiber sample. The process of analyzing PBS by UV–Vis, recording residual volume, and placing fresh PBS on each sample was repeated every three to four days until 13 of 14 samples had no detectable Ibuprofen or 6AN.

A second set of drug release data was generated by processing replicates of the samples used in the previous paragraph prior to evaluating drug release. Samples were aged for one month in a 24 well plate exposed to laboratory air (~20–22 °C and 20–40% relative humidity) and then placed in the cell culture incubator for four hours (temperature 37° C, 5% CO_2). This post-processing method was previously reported by D'Amato *et al.* and was shown to increase the duration of 6AN released from electrospun fibers. Samples were then placed in 500 μL of PBS for two days before analyzing the PBS using UV–Vis, removing remaining volume, and replacing with 500 μL fresh PBS. The process was repeated every three or four days until 13 of the 14 samples had no detectable drug release.

2.4.2. Analysis of drug release data—Drug release from every time point was adjusted to account for evaporation by multiplying the concentration (μg/mL) of drug calculated from the drug quantification algorithm by the final volume of PBS in the well (yielding units of μg). Cumulative release was then calculated for each sample, and release rate was calculated by dividing the amount of drug released into PBS by the number of days PBS was on the sample.

We used a generalized linear model to determine the trends in drug release. The model included quadratic terms with interactions:

$$m_i = \beta_0 + \beta_1[6AN] + \beta_2[Ibu] + \beta_{12}[6AN][Ibu] + \beta_{11}[6AN]^2 + \beta_{22}[Ibu]^2 \quad (3)$$

In Eq. (3), m_i is the mass released or rate of mass release of drug, *i*, from electrospun fibers. The values [6AN][6AN] and [Ibu] are the mass percentages of drug loaded into the electrospun fiber scaffolds. Mass percentages were normalized by subtracting 5% from the loading percentage and dividing by 2.5%, so that control samples had a value of 0 for both

[6AN] and [Ibu] while linear effects samples had values of ± 1 and second order effects groups had values of 0 or ± $\sqrt{2}$. A linear regression was used to determine the values of coefficients. Then the model was refined by removing coefficients that were not statistically significant. Statistical significance of the model with and without a coefficient was determined using an F-test of the model with and without the coefficient. This method is also known as a linear hypothesis test and determines whether the model fit with and without a coefficient significantly alters how well the model fits the data. If there is a significant difference in how the model fits the data when the value is present or removed, then it is concluded that the coefficient makes a significant contribution to the model. This method removes values that are insignificant, ensuring a good fit between the model and data with the fewest number of terms.

The model in Eq. (3) was fit separately to 6AN release and Ibuprofen cumulative release at day two and the final release day. Fitting the data to the first release time point helped us determine how drug loading altered burst release of drug and fitting the data to the final release time point allowed us to see how the total amount of drug released was altered by drug loading. The model in Eq. (3) was also fit to the drug release rate for each time point to track how each component of the model changed drug release rate over time.

2.5. Scanning electron microscopy

Scanning electron microscopy (SEM) was carried out on an AMRAY 1910 field emission SEM using SemTech Solutions X-Stream image capture software. Samples were coated with gold using a Polaron sputter coater. Five images of each sample were collected.

2.6. Characterization of electrospun fibers

Electrospun fiber diameter and linear density (fibers per mm of scaffold) was assessed using the methods described by Hotaling et al. (2015). To identify the location of electrospun fibers in the image, images were passed through a deep neural network trained to segment electrospun fibers. The segmented images were then processed according to Hotaling *et al*, where segmented images of electrospun fibers were skeletonized and a distance transform was used to determine fiber diameter. Fiber density was then determined by counting the number of fibers crossing a horizontal line drawn through the center of the image. All code to characterize electrospun fibers was written in Matlab.

2.7. Statistics

Evaluation of the drug detection method on defined mixtures of drug involved computing R^2 values, where the predicted values were compared to actual values rather than a regression line. For electrospun fiber diameter, a mixed effects negative binomial regression was used to determine the effects of drug loading on fiber diameter. The regression factors were the same as in Eq. (3)) except the random effects of each sample were included in the model. A linear model using Eq. (3) was constructed to determine the effects of drug loading on fiber density. The significance of model components were determined by an F-test. Coefficients were considered weakly significant if $p < 0.05$, and strongly significant if $p < 0.001$. The p-values were used in accordance with the work of Johnson (Johnson, 2013), who demonstrated that a p-value of 0.05 corresponds to a 1:3 or 1:4 likelihood of randomly

obtaining a similar result while a p-value of 0.001 corresponds to a 1:100 or 1:200 likelihood of randomly obtaining a similar result.

3. Results

3.1. Quantification of multiple drugs from UV–Vis spectra

The method of quantifying multiple drug release from electrospun fibers was validated by calculating the amount of ibuprofen and 6AN released from electrospun fiber samples containing only 6AN or only ibuprofen. The expectation was that ibuprofen should not be detected in electrospun fibers containing only 6AN, and 6AN should not be detected in electrospun fibers containing only Ibuprofen. While evaluating drug release from electrospun fibers, an unknown signal was observed in the UV–Vis spectra of PBS samples exposed to electrospun fibers containing only 6AN.

We hypothesized that the unknown signal could be components leached from the disposable, medical grade syringes used for electrospinning (subsequently referred to as syringe components). UV–Vis analysis of a 70% ethanol solution exposed to the syringes for 1 week revealed a signal that decreased in magnitude as the solution was further diluted in 70% ethanol (Fig. 2). The method to detect wavelength-dependent mass absorptivity was used to characterize serial dilutions of syringe components. Then, we analyzed PBS samples exposed to electrospun fibers containing only 6AN or only ibuprofen. In the first round of analysis, Eq. (1) was solved for both 6AN and Ibuprofen concentration without accounting for syringe components (−Syringe). In the second round of analysis, Eq. (1) was solved for 6AN, Ibuprofen, and syringe component concentrations (+ Syringe). When drug release from electrospun fibers that contained only 6AN was determined without accounting for syringe components, the algorithm detected both ibuprofen and 6AN were detected in PBS (Fig. 2b). When syringe components were included in the process of solving Eq. (1), no ibuprofen was detected (as expected) except a nominal amount at Day 15 (< 1 μg). In contrast, when syringe components were excluded from analysis of the fibers containing only Ibuprofen, the algorithm only detected ibuprofen in PBS exposed to ibuprofen fibers (Fig. 2c). When syringe components were accounted for in the analysis, the calculated amount of ibuprofen released from the fibers drastically decreased (272% decrease). These results led us to conclude that inclusion of unknown syringe components into the drug detection algorithm was required to prevent false detection of Ibuprofen release from electrospun fibers. False detection of Ibuprofen was likely due to the overlap between the Ibuprofen spectra (Fig. 1d) and the spectra of the syringe components (Fig. 2a).

Next, we calculated the amount of 6AN, Ibuprofen, and syringe components in serial dilutions of each drug to verify that inclusion of syringe components in our drug detection method did not interfere with accurate calculation of drug concentration. The expectation was that only 6AN would be detected in the 6AN standard curve samples, only Ibuprofen would be detected in the Ibuprofen standard curve samples, and the amount of drug detected would match the amount of drug in the sample. The amount of 6AN, Ibuprofen, and syringe components detected by the algorithm in the 6AN standard curve revealed a high correlation between calculated 6AN and actual 6AN concentration (R^2 greater than 0.999) with no Ibuprofen detected in any of the spectra (Fig. 2d). Similarly, there was a high correlation

between predicted Ibuprofen and actual Ibuprofen concentration (R^2 greater than 0.999) with no 6AN detected (Fig. 2e). To further demonstrate that inclusion of syringe components did not interfere with detection of drug concentration, we mixed all combinations of the four lowest drug concentrations in the standard curve. The drug detection method was capable of accurately calculating the amount of Ibuprofen and 6AN in each sample ($R^2 = 0.986$ relative to a perfect calculation, Fig. 2f). In the second experiment, we created the same mixtures of Ibuprofen and 6AN with a diluted amount of syringe components added to each well. Calculation of the drug concentrations was slightly worse ($R^2 = 0.929$ relative to a perfect calculation) but were still highly correlated with the actual values (Fig. 2g). These results led us to conclude that inclusion of syringe components when calculating 6AN and Ibuprofen concentrations did not have a significant impact on calculating drug concentration, and that the presence of syringe components in a solution could be accounted for to accurately calculate drug concentration.

3.2. Electrospun fiber characterization

To rule out electrospun fiber diameter and linear density as confounding factors in release profiles for each sample, SEM images of all fiber groups were analyzed (Fig. 3a). The distribution of electrospun fibers fit a negative binomial distribution (Fig. 3b), so a negative binomial regression was performed to determine whether drug loading impacted fiber diameter. Drug loading had a weak impact on fiber diameter (Fig. 3c), with 6AN loading increasing fiber diameter ~4 nm per 1% of 6AN ($p = 0.034$) and ibuprofen loading increasing fiber diameter by about the same amount ($p = 0.026$). For the groups used in this study, this change is approximately 1–2 pixels between groups with different concentrations of each drug (10.4–20.8 nm). Analysis of fiber density using a linear regression model did not show any factors to be statistically significant. Based on these results, our conclusion is that changes in the fiber diameter and fiber density caused by differences in drug loading would not have a significant impact on differences in the drug release profiles.

3.3. Simultaneous release of Ibuprofen and 6AN from electrospun fibers

The primary purpose of this study is to understand how the release of multiple drugs is dependent on the concentration of each drug. Fig. 4a shows the design space of our CCC experimental design and shows how 6AN and Ibuprofen release varied with each drug's concentration around the center point of 5% 6AN and 5% Ibuprofen loading (inverted black triangle in Fig. 4b). Drug release was analyzed for 19 days, since day 19 was the first day where none of the samples released any drug. Six replicates of control samples were electrospun (5% 6AN, 5% Ibuprofen), but one sample was removed from analysis because it was a statistical outlier relative to the other samples. The outlier was excluded because it released twice as much 6AN and Ibuprofen than the group mean and more than three standard deviations higher than the group mean. All control samples released both 6AN and ibuprofen (Fig. 4b). Control samples released 0.902 ± 0.075 μg/mL total 6AN (mean ± 95% CI) and 0.451 ± 0.206 μg/mL total Ibuprofen (mean ± 95% CI) over 19 days of release. Fig. 4c shows release rate, which is the drug release observed for that day divided by the number of days the PBS was exposed to the fibers. The release rates show that the fibers released 6AN for up to 9 days and Ibuprofen for up to 5 days, except for one sample that released Ibuprofen at day 16.

Analysis of the remaining experimental groups revealed trends in the drug release profiles of each drug as the loading concentration changed. Both groups with 7.5% 6AN released a total amount of 6AN that was similar to each other, and these samples released more 6AN than all control samples (Fig. 4d, dark orange diamonds and triangles). Similarly, groups with 2.5% 6AN released a total amount of 6AN similar to each other, and these samples released less 6AN than all control samples (Fig. 4d, light orange circles and squares). Each of the groups containing 7.5% 6AN had a different amount of Ibuprofen loaded into the fibers (2.5% or 7.5% ibuprofen) so ibuprofen loading appeared to have little effect on 6AN release from the fibers. The same was true for fibers loaded with 2.5% 6AN. The same trends were observed for Ibuprofen release, where samples containing 7.5% Ibuprofen (Fig. 4d, dark green circles and diamonds) and 2.5% Ibuprofen (Fig. 4d, light green squares and triangles) released more or less Ibuprofen respectively compared to controls (5% 6AN and 5% ibuprofen). For the second order effects groups, total 6AN release correlated with initial loading of either 6AN or Ibuprofen. Samples containing 8.54% (Fig. 4e, dark orange circles) or 1.46% 6AN (Fig. 4e, light orange diamonds) released the largest and smallest total mass of 6AN respectively. Similarly, samples containing 5% 6AN released more or less 6AN with respect to Ibuprofen loading of 8.54% (Fig. 4e, dark green squares) or 1.46% (Fig. 4e, light green triangles). The sample containing 5% Ibuprofen and 8.54% 6AN released a higher mass of Ibuprofen compared to controls (Fig. 4e, green circles) and the sample containing 5% Ibuprofen and 1.46% 6AN released a similar amount of Ibuprofen compared to controls. The results of this experiment show that each drug releases from the fibers with respect to loading concentration, but there is some evidence that both drugs release with respect to the other drugs loading concentration as well.

To elucidate the relationships between each drug's release profile on initial loading concentrations, linear models were fit to the drug release data. The components of the linear models were the initial drug loading concentrations. First, we fit the model (Eq. (3)) to drug release at two days (the first release time point), with separate models for 6AN release and Ibuprofen release. Fig. 5a is a plot of the coefficients for each of the model components when fit to the 6AN day 2 release data (orange points) and fit to the Ibuprofen day 2 release data (green points). The intercept values in the model represent the drug released from control samples (5% 6AN and 5% Ibuprofen), and other values represent how drug release changes with 6AN and Ibuprofen loading relative to control samples. Evaluation of the model revealed that 6AN burst release is weakly dependent on Ibuprofen loading concentration ($p = 0.043$) and 6AN loading concentration ($p = 0.011$). In contrast, Ibuprofen burst release was not dependent on 6AN loading, but was strongly dependent on Ibuprofen loading concentration ($p < 0.001$) and weakly dependent on the square of Ibuprofen loading concentration ($p = 0.00743$). These trends are evident in a surface plot of each model within the experimental space. The surface of the 6AN burst release model (Fig. 5b) showed an increase in 6AN release as 6AN loading increases and as Ibuprofen loading increases. However, the surface of the Ibuprofen burst release model (Fig. 5c) only changes with respect to the Ibuprofen axis. Similar trends were observed when the total mass of 6AN or Ibuprofen release at day 19 were fit to the model (Fig. 5d). Total 6AN release was strongly dependent on 6AN concentration ($p < 0.001$), and weakly dependent on Ibuprofen concentration ($p = 0.0228$) and the square of 6AN concentration ($p = 0.0247$). Total

Ibuprofen concentration was only dependent on Ibuprofen concentration ($p < 0.001$). As with the burst release model, the surface of the 6AN total release model shows how total 6AN release is dependent on both 6AN and Ibuprofen concentration (Fig. 5e). The surface of the Ibuprofen model shows how total Ibuprofen release is only dependent on Ibuprofen concentration (Fig. 5f). Overall, the results of the burst and total release models reveal that 6AN release from electrospun fibers is dependent on the initial loading concentration of 6AN and Ibuprofen, while Ibuprofen release is only dependent on Ibuprofen loading concentration.

3.4. Extended release of multiple factors from electrospun fibers

Work by D'Amato *et al.* showed that post-processing electrospun fibers could change the release profile of 6AN (D'Amato et al., 2017), so we investigated whether post-processing caused a difference in how drug loading affected drug release. D'Amato *et al.* were able to extend the release of 6AN (more than 30 days of release) from electrospun fibers by aging electrospun fibers for 28 days followed by a 4 h incubation in a cell culture incubator at 37 °C and 90–95% relative humidity prior to evaluating the release of 6AN from the fibers. The rationale for the change in the drug release curve was that residual solvent (HFP) left over from the electrospinning process altered the release of drug from the fibers. These results led us to hypothesize that the release of multiple drugs from a single set of fibers might also be impacted by retained solvent, so we re-evaluated the release of Ibuprofen and 6AN after the fibers were aged for 1 month and incubated in our cell culture incubator for 4 h.

The drug release profile of the control samples (Fig. 6A) revealed similarities and differences with the previous set of release curves. 6AN release was observed for up to 13 days (Fig. 6B, orange points), and Ibuprofen release was also observed for up to 13 days (Fig. 6B, green points). The total release of 6AN from control samples was 0.988 ± 0.143 μg/mL (mean ± 95% CI) and the total release of Ibuprofen was 0.228 ± 0.258 μg/mL (mean ± 95% CI). These results show that there is a marginal increase (~10%) in the total amount of 6AN released after aging the fibers and treating in a cell culture incubator compared to no aging or incubation, and the 6AN was released over a slightly longer time. In contrast, the amount of Ibuprofen released decreased by nearly 50%, but the release was extended when the fibers were post-processed (13 days versus 5 days).

Qualitative analysis of the linear effects groups revealed treated samples containing 7.5% 6AN and 7.5% Ibuprofen (Fig. 6c, orange diamonds) or 2.5% Ibuprofen (Fig. 6c, orange triangles) released more or less 6AN depending on Ibuprofen concentration. The same trend existed for samples containing 2.5% 6AN, where treated samples that contained 7.5% Ibuprofen (Fig. 6c, light orange circles) or 2.5% Ibuprofen (Fig. 6c, light orange squares) released more or less 6AN depending on Ibuprofen concentration. Samples that contained 7.5% Ibuprofen were similarly affected by 6AN loading, where the sample containing 7.5% Ibuprofen and 7.5% 6AN (Fig. 6c, dark green diamonds) or 2.5% 6AN (Fig. 6c, dark green circles) released more or less Ibuprofen with respect to 6AN loading concentration. Samples containing 2.5% Ibuprofen did not release any detectable amount of Ibuprofen at any time point. For the second order effects groups, the samples that contained 8.54% 6AN (Fig. 6d, dark orange circles) or 1.46% 6AN (Fig. 6d, light orange diamonds) released the largest or

smallest amounts of 6AN respectively. Similarly, the samples containing 8.54% Ibuprofen (Fig. 6d, dark green squares) released more Ibuprofen than any other second order effects group and the fibers containing 1.46% Ibuprofen (Fig. 6d, light green triangles) Ibuprofen released no detectable Ibuprofen. The second order effects samples containing 5% 6AN and 8.54% Ibuprofen (Fig. 6d, orange squares) or 1.46% Ibuprofen (Fig. 6d, orange triangles) released more or less 6AN with respect to Ibuprofen concentration. For Ibuprofen release, samples containing 5% Ibuprofen and 8.54% 6AN released more Ibuprofen (Fig. 6d, green circles) than controls, and the sample containing 5% Ibuprofen and 1.46% 6AN released a similar amount of drug compared to controls (Fig. 6d, green diamonds). By visual inspection, these results suggest that post processing of electrospun fibers alters the release characteristics of each drug when visually compared to the drug release data from Fig. 3. A more detailed discussion of the differences is presented in the discussion (Section 4.2).

The release data of treated samples were fit to Eq. (3), and the results confirmed that post-processing treatment altered each drug's release profile. The 6AN burst release model (Fig. 6a, orange circles) revealed 6AN release at two days was strongly dependent on 6AN loading concentration ($p < 0.001$) and Ibuprofen loading concentration ($p < 0.001$), and weakly dependent on the square of 6AN concentration ($p = 0.0182$). The Ibuprofen burst release model (Fig. 7a, green circles) revealed Ibuprofen release at day 2 was only dependent on Ibuprofen concentration ($p < 0.001$). As with the untreated samples, the surface of the 6AN burst release model (Fig. 7b) is dependent on both 6AN and Ibuprofen concentration and the surface of the Ibuprofen burst release model (Fig. 7c) is only dependent on Ibuprofen concentration. Like the 6AN burst release model, the 6AN total release model (Fig. 7d, orange circles) showed a strong dependence on 6AN loading concentration ($p < 0.001$) and Ibuprofen concentration ($p < 0.001$), and a weak dependence on the square of 6AN concentration ($p = 0.00357$). The total release model for Ibuprofen (Fig. 7d, green circles) was also strongly dependent on Ibuprofen loading concentration ($p < 0.001$) and unlike the untreated samples, there was a weak dependence on 6AN loading concentration. The surface of the 6AN total release model (Fig. 7e) and the surface of the Ibuprofen total release model (Fig. 7f) both showed the dependence on 6AN and Ibuprofen. These results indicate that post-processing had a significant effect on drug release, especially the impact of each drug's loading concentration on drug release.

4. Discussion

To briefly summarize the findings of this study, we (i) validated a method to robustly quantify the concentrations of multiple drugs in a sample, (ii) established that loading two different drugs into electrospun fibers can affect the drug release profile of each drug, and (iii) that post-processing electrospun fibers can change drug release profiles when multiple drugs are loaded into electrospun fibers. Electrospun fibers have been of increasing interest for regenerative medicine and tissue engineering as a biomimetic tool to supply a fibrillar physical cue to cells. In addition to the support and guidance of cells, they can be used to release pharmaceuticals to aid in regeneration. However, much of the literature to this point have focused on the release of a single agent. Therefore, the endeavor of this work was to investigate how loading multiple drugs into a single set of electrospun fibers alters the release profile of each drug. A better understanding of how multiple drugs loaded into a

single set of electrospun fibers alter release profiles will help meet the increasing complexity of new tissue engineering approaches. While the results of our experiments can be complicated to explicate at the level of individual sample comparisons, our approach provides a way of understanding how an individual drug release profile is affected by loading other drugs into a single set of electrospun fibers as the initial drug loading concentrations vary. Use of this systematic approach to release multiple drugs from electrospun fibers demonstrates the capacity of electrospun fibers to meet the increasing demands of tissue engineering and regenerative medicine.

4.1. Detection of multiple drugs from UV–Vis spectra

UV–Vis is commonly used to detect drug release from electrospun fibers, but in many cases only a single wavelength is used to measure absorbance. If only one drug is expected to be in a sample, then absorbance at a single wavelength is sufficient to determine drug concentration. However, use of a single wavelength for absorbance may hide unexpected background offsets or other unexpected components in a sample. This was made clear in the present study, where we discovered an unknown signal in the drug release profiles of electrospun fiber samples containing only one drug. A survey of the literature revealed at least one other group found something similar, where hippocampal neuron viability and neurite formation/extension were negatively affected when exposed to cell culture medium delivered from medical grade, sterile, disposable syringes (Woo et al., 2014). We did not attempt to determine the identity of the components in our electrospinning syringes since it was beyond the scope of this study, but it was clear that the syringe components were interfering with our ability to characterize drug release. This finding suggests that studies using electrospun fibers for drug release may have had similar contaminants since disposable medical grade syringes are commonly used for electrospinning in tissue engineering research. The presence of contaminants may have amplified the observed drug release if drug was detected by a single UV–Vis wavelength. This is true for the study by D'Amato et al., where 6AN release from electrospun fibers was assessed by measuring absorbance at 267 nm. Absorbance at 267 nm is well within the absorbance spectrum of the syringe components measured in this study (Fig. 2a). However, since no attempts were made to identify the unknown components released from the fibers, these findings may be limited to this study or studies that use disposable plastic syringes.

The discovery of the unknown syringe components and capacity to account for the new signals demonstrate the robustness of the method we developed in this study as well as the need for appropriate control samples. For the electrospun fiber sample containing only 6AN, ibuprofen was likely reported by the drug detection algorithm because of the significant overlap between the Ibuprofen spectrum (Fig. 1d) and the syringe components (Fig. 2a), but less overlap between syringe components and the 6AN spectrum (Fig. 1c). This also explains why a larger quantity of Ibuprofen was detected in the electrospun fiber scaffold containing only Ibuprofen before accounting for syringe components (Fig. 2c). Further, the overlap in the signal between the syringe components and Ibuprofen likely accounts for the marginally worse detection of Ibuprofen in mixtures of 6AN and Ibuprofen when syringe components are added to the mixture (Fig. 2g). Due to the overlap in signal, it would be reasonable to use a different method of quantifying drug release, such as liquid

chromatography-mass spectrometry (LCMS). Measuring drug release with LCMS is likely be more robust than the method developed here, but LCMS is more time consuming and costly with respect to UV–Vis. Since one goal of this work is to develop a methodology to loading multiple drugs into electrospun fibers, it is feasible to consider situations when 3 or more drugs might be loaded into the fibers. The design space we use here grows exponentially with the number of drugs loaded into the fibers, making the rapid analysis developed here desirable for determining drug release since UV–Vis is rapid. The method developed here was shown to differentiate between three signals in a UV–Vis spectrum (ibuprofen, 6AN, and syringe components) including two signals that had significant overlap (ibuprofen and syringe components). This method will aid in future studies to quantify the release of multiple drugs.

4.2. Factors influencing multiple drugs release from electrospun fibers

The primary goal of this work was to develop an approach to study the release of multiple drugs from slowly degrading electrospun fibers. A large body of literature has focused on the release of drug from electrospun fibers, (Hu et al., 2014; Chou et al., 2015; Jang et al., 2009; Sill and von Recum, 2008; Ji et al., 2011; Szentivanyi et al., 2011; Chakraborty et al., 2009; Hadjiargyrou and Chiu, 2008) and multiple factors that affect drug release have been identified. Factors that have been studied include hydrophobicity/hydophilicity of the drug (Zeng et al., 2005) and electrospun fiber diameter (Chen et al., 2012). One factor that is commonly mentioned but poorly investigated in the electrospun fiber drug delivery literature are physicochemical interactions between drugs and polymers. It is expected that a favorable interaction between a drug and polymer would cause the drug to diffuse out of the polymer more slowly. Addition of multiple drugs into a single set of electrospun fibers may exponentially increase the number of physicochemical interactions involved in drug diffusion from a polymer, and the addition of new interactions may lead to different release profiles. Thakur *et al.* demonstrated that simultaneous release of lidocaine and mupirocin from electrospun PLLA fibers led to a change in the drug release profile of mupirocin compared to an electrospun fiber mat where individual fibers contained either lidocaine or mupirocin (Johnson, 2013). The cause of the mupirocin burst release was the formation of crystalline mupirocin domains within the fiber. The study by Thakur *et al.* only investigated the binary example of releasing drugs from the same or separate fibers, so it was unclear how much of the burst release was caused by lidocaine versus mupirocin concentration or how the release changed with each drug's concentration. It might be expected that use of different drugs might lead to different release profiles, since each drug has unique physicochemical interactions with itself, other drugs, and the polymer it is encapsulated in. To our knowledge, Thakur's study is the only study that has investigated the diffusion of multiple small drugs from slowly degrading electrospun fibers, and we found no analysis in the literature that evaluated the release of multiple drugs as a function of loading concentration.

In this study we analyze drug release with a standard linear model with second order terms and interactions rather than a model built upon first principles, and the components of the model may be interpreted in multiple ways. One way the model can be interpreted is within the context of physicochemical mechanisms of multi-drug release. Briefly, i) the linear

components (i.e. [6AN] and [Ibu] in Eq. (1)) may be associated with each drugs affinity for the polymer, ii) the interaction parameter ([6AN][Ibu][6AN][Ibu]) may be associated with the physicochemical interaction between 6AN and Ibuprofen, iii) and the square components ($[6AN]^2$ and $[Ibu]^2$) may be associated with the physicochemical interactions between each drug with itself. For the linear effects, if one drug has a lower affinity for a polymer than a second drug, the addition of the second drug to electrospun fibers could exclude the first drug from associating with the polymer and cause more of the first drug to be released. With this interpretation of the model, 6AN would have a lower affinity for PLLA relative to Ibuprofen since Ibuprofen appears in the 6AN release models while 6AN does not appear in the Ibuprofen release models (Fig. 5). Further evidence of 6AN having a lower affinity for PLLA than Ibuprofen is the smaller total weight of Ibuprofen released across all samples relative to the total 6AN released. However, these observations may be confounded by the differences in molecular weight between the drugs, since Ibuprofen (203 g/mol) has a larger molecular weight than 6AN (137 g/mol). The absence of the drug interaction parameter from all models might indicate 6AN and Ibuprofen have little affinity for each other. The remaining components of the model ($[6AN]^2$ and $[Ibu]^2$) may be interpreted as a drug's affinity for itself. The lack of squared components in most of the models suggest that drug interactions with itself likely did not contribute to the results observed in this study. Associating the components of the model with physicochemical interactions between drugs and the polymer aid in understanding the underlying principles that are being modeled, but additional work should be performed to determine whether this model is describing a physicochemical mechanism or another process.

The model used in this study may be describing confounding factors related to drug loading in electrospun fibers other than physicochemical interactions. For example, it is known that adding drug to electrospun fibers tends to cause a decrease in fiber diameter (Schaub and Gilbert, 2011) likely due to an increase in charge density (where increased charge density results in smaller diameter fibers) (Fong et al., 1999). Since smaller fibers lead to more drug release (Chen et al., 2012), it is possible that fiber diameter is a confounding factor. To account for this, we quantified fiber diameter to remove this as a confounding factor (Fig. 3). Although there may be other confounding factors, our models tended to be accurate (most models had an adjusted $R^2 > 0.8$).

The most striking discovery in our experiments was the shift in Ibuprofen release from being independent of 6AN loading concentration (Fig. 5f) to dependent on 6AN loading concentration (Fig. 7f) after electrospun fibers were treated as described by D'Amato *et al* (D'Amato et al., 2017). The study by D'Amato and colleagues found that aging electrospun PLLA fibers loaded with 6AN for 1 month followed by a 4-hour incubation in a cell culture incubator caused 6AN release to extend to more than 44 days compared to 9 days of release without treatment. Their explanation for the change in 6AN release was that residual electrospinning solvent (HFP) was removed by the aging and incubation treatment. It is known that electrospinning solvents can remain in electrospun fibers for up to one month post-electrospinning at concentrations of 5% or more (D'Amato et al., 2017), therefore removal of solvent from the electrospun fibers might reduce the free volume within the fibers (decreasing the rate of diffusion) (D'Amato et al., 2017). In the context of the physicochemical discussion presented in this manuscript, another explanation is that the

HFP interacts with the polymer and the drug. Removal of the solvent permits more interaction between the drug and polymer (resulting in slower diffusion) or leads to an increase in total drug release if the drug and polymer do not interact favorably. The physiochemical explanation is supported by the evidence in our study, where aging and incubation of electrospun fibers led to an increase in total 6AN release (also observed by D'Amato *et al.*) and a decrease in Ibuprofen release from control samples. This explanation implies 6AN interacts less favorably and Ibuprofen more favorably with PLLA. The increase in release duration could then be explained by the decrease in free volume. One discrepancy we found between our study and the study by D'Amato and colleagues was that 6AN release was extended 5-fold with treatment (from 9 days to 44 days) where we only saw a marginal increase in 6AN release (9–13 days) and Ibuprofen (5–13 days). This discrepancy may be explained by our use of multiple drugs versus their use of a single drug but could also be explained by their method of quantifying drug release. D'Amato *et al.* only used a single wavelength to quantify release (267 nm) that was within the absorption spectrum of the syringe components we observed in this study (and they used the same type of syringes used in our study). Therefore, it is unclear how much of the drug release they observed was from the 6AN versus the syringe components leaching from the fibers, since treatment of the fibers may change how syringe components are released from the fibers. Regardless, the work presented here confirms that their post-processing treatment has a significant impact on how drug is released.

The work presented in this study demonstrates the capacity to model the release of multiple drugs from electrospun fibers, providing a new opportunity to engineer drug release. There are drug loading concentrations in the total drug release models for 6AN (Fig. 7e) and Ibuprofen (Fig. 7f) that have similar total release but different values in the burst release models at the corresponding drug loading concentrations (Fig. 7b and c for 6AN and Ibuprofen respectively). This could permit engineering of drug release profiles when multiple drugs are loaded into a single mat of electrospun fibers, where a larger or smaller burst release of drug can be selected while releasing the same total amount of drug. Future work will use a combination of statistical modeling demonstrated in this manuscript and post-processing fibers to engineer the release of multiple drugs to meet the needs of increasingly complex approaches to tissue engineering.

5. Conclusions

We developed a robust method of detecting multiple drug concentrations in a solution of PBS. Application of this method to drug release from electrospun fibers led to the discovery of unknown components released from electrospun fibers, and the unknown components were determined to be chemicals leached from syringes during the electrospinning process. Analysis of multi-drug release from electrospun fibers revealed that drug release profiles for 6AN were dependent on the amount of 6AN loaded into the fibers (as expected) and on the amount of Ibuprofen loaded into the fibers. In contrast, Ibuprofen release was only dependent on the amount of Ibuprofen loaded into the fibers. Post-processing of electrospun fibers according to the method described by D'Amato *et al.* (one-month aging and annealing at 37 °C) caused Ibuprofen release to become dependent on both Ibuprofen and 6AN loading concentration. These results indicate the ability to alter drug release profiles by loading

multiple drugs into the same electrospun fiber mat, providing an additional tool to engineer the release of multiple drugs from electrospun fibers.

Supplementary Material

Refer to Web version on PubMed Central for supplementary material.

Acknowledgements

We wish to thank the following funding agencies for their support of this work and our personnel: VA Rehab R&D SPiRE award to Joseph M Corey (I21-RX001904) and the National Institute of Dental and Craniofacial Research at NIH awarded to Nicholas J Schaub (2T32DE007057-41). The authors would like to thank Allison Grant and Shuqing Zhang for meticulous comments on the content of the paper.

References

Alvarez-Perez MA, Guarino V, Cirillo V, Ambrosio L, 2010 Influence of gelatin cues in PCL electrospun membranes on nerve outgrowth. Biomacromolecules 11, 2238–2246. 10.1021/bm100221h. [PubMed: 20690634]

Cao H, Liu T, Chew SY, 2009 The application of nano fibrous scaffolds in neural tissue engineering. Adv. Drug Deliv. Rev 61, 1055–1064. 10.1016/j.addr.2009.07.009. [PubMed: 19643156]

Chakraborty S, Liao I-C, Adler A, Leong KW, 2009 Electrohydrodynamics: A facile technique to fabricate drug delivery systems. Adv. Drug Deliv. Rev 61, 1043–1054. 10.1016/j.addr.2009.07.013. [PubMed: 19651167]

Chen SC, Huang XB, Cai XM, Lu J, Yuan J, Shen J, 2012 The influence of fiber diameter of electrospun poly(lactic acid) on drug delivery. Fibers Polym. 13, 1120–1125. 10.1007/s12221-012-1120-x.

Chew SY, Mi R, Hoke A, Leong KW, 2007 Aligned protein-polymer composite fibers enhance nerve regeneration: a potential tissue-engineering platform. Adv. Funct. Mater 17, 1288–1296. 10.1002/adfm.200600441. [PubMed: 18618021]

Chou S-F, Carson D, Woodrow KA, 2015 Current strategies for sustaining drug release from electrospun nanofibers. J. Control. Release 220, 584–591. 10.1016/j.jconrel.2015.09.008. [PubMed: 26363300]

Corey JM, Lin DY, Mycek KB, Chen Q, Samuel S, Feldman EL, et al., 2007 Aligned electrospun nanofibers specify the direction of dorsal root ganglia neurite growth. J. Biomed. Mater. Res. A 83A, 636–645. 10.1002/jbm.a.31285.

Corey JM, Gertz CC, Wang B-S, Birrell LK, Johnson SL, Martin DC, et al., 2008 The design of electrospun PLLA nanofiber scaffolds compatible with serum-free growth of primary motor and sensory neurons. Acta Biomater. 4, 863–875. 10.1016/j.actbio.2008.02.020. [PubMed: 18396117]

Cregg JM, DePaul MA, Filous AR, Lang BT, Tran A, Silver J, 2014 Functional regeneration beyond the glial scar. Exp. Neurol 253, 197–207. 10.1016/j.expneurol.2013.12.024. [PubMed: 24424280]

D'Amato AR, Schaub NJ, Cardenas JM, Franz E, Rende D, Ziemba AM, et al., 2017 Evaluation of procedures to quantify solvent retention in electrospun fibers and facilitate solvent removal. Fibers Polym. 18, 483–492. 10.1007/s12221-017-1061-5.

D'Amato AR, Schaub NJ, Cardenas JM, Fiumara AS, Troiano PM, Fischetti A, et al., 2017 Removal of retained electrospinning solvent prolongs drug release from electrospun PLLA fibers. Polymer 123, 121–127. 10.1016/j.polymer.2017.07.008. [PubMed: 29200507]

Dill J, Patel AR, Yang X-L, Bachoo R, Powell CM, Li S, 2010 A molecular mechanism for ibuprofen-mediated RhoA inhibition in neurons. J. Neurosci 30, 963–972. 10.1523/JNEUROSCI.5045-09.2010. [PubMed: 20089905]

Fong H, Chun I, Reneker DH, 1999 Beaded nanofibers formed during electrospinning. Polymer 40, 4585–4592. 10.1016/S0032-3861(99)00068-3.

Fu Q, Hue J, Li S, 2007 Nonsteroidal anti-inflammatory drugs promote axon regeneration via RhoA inhibition. J. Neurosci 27, 4154–4164. 10.1523/JNEUROSCI.4353-06.2007. [PubMed: 17428993]

Gelain F, Panseri S, Antonini S, Cunha C, Donega M, Lowery J, et al., 2011 Transplantation of nanostructured composite scaffolds results in the regeneration of chronically injured spinal cords. ACS Nano 5, 227–236. 10.1021/nn102461w. [PubMed: 21189038]

Gertz CC, Leach MK, Birrell LK, Martin DC, Feldman EL, Corey JM, 2010 Accelerated neuritogenesis and maturation of primary spinal motor neurons in response to nanofibers. Dev. Neurobiol 70, 589–603. 10.1002/dneu.20792. [PubMed: 20213755]

Hadjiargyrou M, Chiu JB, 2008 Enhanced composite electrospun nanofiber scaffolds for use in drug delivery. Expert. Opin. Drug Deliv 5, 1093–1106. 10.1517/17425247.5.10.1093. [PubMed: 18817515]

Haghighat N, McCandless DW, 1997 Effect of 6-aminonicotinamide on metabolism of astrocytes and C6-glioma cells. Metab. Brain Dis 12, 29–45. 10.1007/BF02676352. [PubMed: 9101536]

Holzwarth JM, Ma PX, 2011 Biomimetic nanofibrous scaffolds for bone tissue engineering. Biomaterials 32, 9622–9629. 10.1016/j.biomaterials.2011.09.009. [PubMed: 21944829]

Hotaling NA, Bharti K, Kriel H, Simon CG Jr., 2015 DiameterJ: A validated open source nano fiber diameter measurement tool. Biomaterials 61, 327–338. 10.1016/j.biomaterials.2015.05.015. [PubMed: 26043061]

Hu X, Liu S, Zhou G, Huang Y, Xie Z, Jing X, 2014 Electrospinning of polymeric nano fibers for drug delivery applications. J. Control. Release 185, 12–21. 10.1016/j.jconrel.2014.04.018. [PubMed: 24768792]

Hurtado A, Cregg JM, Wang HB, Wendell DF, Oudega M, Gilbert RJ, et al., 2011 Robust CNS regeneration after complete spinal cord transection using aligned poly-l-lactic acid microfibers. Biomaterials 32, 6068–6079. 10.1016/j.biomaterials.2011.05.006. [PubMed: 21636129]

Jang J-H, Castano O, Kim H-W, 2009 Electrospun materials as potential platforms for bone tissue engineering. Adv. Drug Deliv. Rev 61, 1065–1083. 10.1016/j.addr.2009.07.008. [PubMed: 19646493]

Ji W, Sun Y, Yang F, van den Beucken JJJP, Fan M, Chen Z, et al., 2011 Bioactive electrospun scaffolds delivering growth factors and genes for tissue engineering applications. Pharm. Res 28, 1259–1272. 10.1007/s11095-010-0320-6. [PubMed: 21088985]

Jiang X, Lim SH, Mao H-Q, Chew SY, 2010 Current applications and future perspectives of artificial nerve conduits. Exp. Neurol 223, 86–101. 10.1016/j.expneurol.2009.09.009. [PubMed: 19769967]

Johnson VE, 2013 Revised standards for statistical evidence. Proc. Natl. Acad. Sci 110, 19313–19317. 10.1073/pnas.1313476110. [PubMed: 24218581]

Kim Y, Haftel VK, Kumar S, Bellamkonda RV, 2008 The role of aligned polymer fiber-based constructs in the bridging of long peripheral nerve gaps. Biomaterials 29, 3117–3127. 10.1016/j.biomaterials.2008.03.042. [PubMed: 18448163]

Koh HS, Yong T, Chan CK, Ramakrishna S, 2008 Enhancement of neurite outgrowth using nano-structured scaffolds coupled with laminin. Biomaterials 29, 3574–3582. 10.1016/j.biomaterials.2008.05.014. [PubMed: 18533251]

Lambert JH, Anding E (Ernst). Photometrie. Photometria, sive De mensura et gradibus luminis, colorum et umbrae (1760). Leipzig, W. Engelmann; 1892.

Leach MK, Feng Z-Q, Tuck SJ, Corey JM, 2011 Electrospinning fundamentals: optimizing solution and apparatus parameters. J. Vis. Exp 10.3791/2494.

Liao S, Li B, Ma Z, Wei H, Chan C, Ramakrishna S, 2006 Biomimetic electrospun nanofibers for tissue regeneration. Biomed. Mater 1, R45 10.1088/1748-6041/1/3/R01. [PubMed: 18458387]

Liu S, Pan G, Liu G, Neves J. das, Song S, Chen S, et al., 2017 Electrospun fibrous membranes featuring sustained release of ibuprofen reduce adhesion and improve neurological function following lumbar laminectomy. J. Controlled Release 264, pp. 1–13. doi: 10.1016/j.jconrel.2017.08.011.

Liu T, Houle JD, Xu J, Chan BP, Chew SY, 2012 Nanofibrous Collagen nerve conduits for spinal cord repair. Tissue Eng. Part A 18, 1057–1066. 10.1089/ten.tea.2011.0430. [PubMed: 22220714]

Lundborg G, 2003 Nerve injury and repair – a challenge to the plastic brain. J. Peripher. Nerv. Syst 8, 209–226. 10.1111/j.1085-9489.2003.03027.x. [PubMed: 14641646]

Morel P, 2018 Gramm: grammar of graphics plotting in Matlab. J. Open Source Softw 10.21105/joss.00568.

Neal RA, Tholpady SS, Foley PL, Swami N, Ogle RC, Botchwey EA, 2012 Alignment and composition of laminin–polycaprolactone nanofiber blends enhance peripheral nerve regeneration. J. Biomed. Mater. Res. A 100A, 406–423. 10.1002/jbm.a.33204.

Pfister BJ, Gordon T, Loverde JR, Kochar AS, Mackinnon SE, Cullen DK, 2011 Biomedical engineering strategies for peripheral nerve repair: surgical applications, state of the art, and future challenges. Crit. Rev. Biomed. Eng 39 10.1615/CritRevBiomedEng.v39.i2.20.

Pham QP, Sharma U, Mikos AG, 2006 Electrospinning of polymeric nanofibers for tissue engineering applications: a review. Tissue Eng. 12, 1197–1211. 10.1089/ten.2006.12.1197. [PubMed: 16771634]

Poggendorff JC, Annalen der Physik JA Barth; 1852.

Politis MJ, 1989 6-Aminonicotinamide selectively causes necrosis in reactive astroglia cells in vivo: Preliminary morphological observations. J. Neurol. Sci 92, 71–79. 10.1016/0022-510X(89)90176-7. [PubMed: 2527969]

Prabhakaran MP, Venugopal J, Chan CK, Ramakrishna S, 2008 Surface modified electrospun nano fibrous scaffolds for nerve tissue engineering. Nanotechnology 19, 455102 10.1088/0957-4484/19/45/455102. [PubMed: 21832761]

Riggin CN, Qu F, Kim DH, Huegel J, Steinberg DR, Kuntz AF, et al., 2017 Electrospun PLGA nanofiber scaffolds release ibuprofen faster and degrade slower after in vivo implantation. Ann. Biomed. Eng 45, 2348–2359. 10.1007/s10439-017-1876-7. [PubMed: 28653294]

Rolofif F, Scheiblich H, Dewitz C, Dempewolf S, Stern M, Bicker G, 2015 Enhanced neurite outgrowth of human model (NT2) neurons by small-molecule inhibitors of Rho/ROCK signaling. PLoS ONE 10 10.1371/journal.pone.0118536.

Schaub NJ, Gilbert RJ, 2011 Controlled release of 6-aminonicotinamide from aligned, electrospun fibers alters astrocyte metabolism and dorsal root ganglia neurite outgrowth. J. Neural Eng 8, 046026 10.1088/1741-2560/8/4/046026. [PubMed: 21730749]

Schaub NJ, Johnson CD, Cooper B, Gilbert RJ, 2015 Electrospun fibers for spinal cord injury research and regeneration. J. Neurotrauma 33, 1405–1415. 10.1089/neu.2015.4165.

Schaub NJ, Le Beux C, Miao J, Linhardt RJ, Alauzun JG, Laurencin D, et al., 2015 The effect of surface modification of aligned poly-L-lactic acid electrospun fibers on fiber degradation and neurite extension. PLoS ONE 10, e0136780 10.1371/journal.pone.0136780. [PubMed: 26340351]

Schaub, n.d. Electrospun fibers: a guiding scaffold for research and regeneration of the spinal cord n.d http://www.nrronline.org/article.asp?issn=1673-5374;year=2016;volume=11;issue=11;spage=1764;epage=1765;aulast=Schaub (accessed December 16, 2016).

Shin S-H, Purevdorj O, Castano O, Planell JA, Kim H-W, 2012 A short review: Recent advances in electrospinning for bone tissue regeneration. J. Tissue Eng 3, 2041731412443530. doi: 10.1177/2041731412443530. [PubMed: 22511995]

Sill TJ, von Recum HA, 2008 Electrospinning: Applications in drug delivery and tissue engineering. Biomaterials 29, 1989–2006. 10.1016/j.biomaterials.2008.01.011. [PubMed: 18281090]

Silver J, Miller JH, 2004 Regeneration beyond the glial scar. Nat. Rev. Neurosci 5, 146–156. 10.1038/nrn1326. [PubMed: 14735117]

Sundararaj SC, Thomas MV, Peyyala R, Dziubla TD, Puleo DA, 2013 Design of a multiple drug delivery system directed at periodontitis. Biomaterials 34, 8835–8842. 10.1016/j.biomaterials.2013.07.093. [PubMed: 23948165]

Szentivanyi A, Chakradeo T, Zernetsch H, Glasmacher B, 2011 Electrospun cellular microenvironments: Understanding controlled release and scaffold structure. Adv. Drug Deliv. Rev 63, 209–220. 10.1016/j.addr.2010.12.002. [PubMed: 21145932]

Thakur RA, Florek CA, Kohn J, Michniak BB, 2008 Electrospun nanofibrous polymeric scaffold with targeted drug release profiles for potential application as wound dressing. Int. J. Pharm 364, 87–93. 10.1016/j.ijpharm.2008.07.033. [PubMed: 18771719]

Venugopal J, Low S, Choon AT, Ramakrishna S, 2008 Interaction of cells and nanofiber scaffolds in tissue engineering. J. Biomed. Mater. Res. B Appl. Biomater 84B, 34–48. 10.1002/jbm.b.30841.

Wang X, Ding B, Li B, 2013 Biomimetic electrospun nanofibrous structures for tissue engineering. Mater. Today 16, 229–241. 10.1016/j.mattod.2013.06.005.

Wang HB, Mullins ME, Cregg JM, Hurtado A, Oudega M, Trombley MT, et al., 2009 Creation of highly aligned electrospun poly-L-lactic acid fibers for nerve regeneration applications. J. Neural Eng 6, 016001 10.1088/1741-2560/6/1/016001. [PubMed: 19104139]

Wang HB, Mullins ME, Cregg JM, McCarthy CW, Gilbert RJ, 2010 Varying the diameter of aligned electrospun fibers alters neurite outgrowth and Schwann cell migration. Acta Biomater. 6, 2970–2978. 10.1016/j.actbio.2010.02.020. [PubMed: 20167292]

Woo Lee Tet, Sergey Tumanov, Villas-Bôas Silas G, Montgomery Johanna M, Birch Nigel P., 2014 Chemicals eluting from disposable plastic syringes and syringe filters alter neurite growth, axogenesis and the microtubule cytoskeleton in cultured hippocampal neurons. J. Neurochem 133, 53–65. 10.1111/jnc.13009.

Yang F, Murugan R, Ramakrishna S, Wang X, Ma Y-X, Wang S, 2004 Fabrication of nano-structured porous PLLA scaffold intended for nerve tissue engineering. Biomaterials 25, 1891–1900. 10.1016/j.biomaterials.2003.08.062. [PubMed: 14738853]

Zeng J, Xu X, Chen X, Liang Q, Bian X, Yang L, et al., 2003 Biodegradable electrospun fibers for drug delivery. J. Control. Release 92, 227–231. 10.1016/S0168-3659(03)00372-9. [PubMed: 14568403]

Zeng J, Yang L, Liang Q, Zhang X, Guan H, Xu X, et al., 2005 Influence of the drug compatibility with polymer solution on the release kinetics of electrospun fiber formulation. J. Control. Release 105, 43–51. 10.1016/j.jconrel.2005.02.024. [PubMed: 15908033]

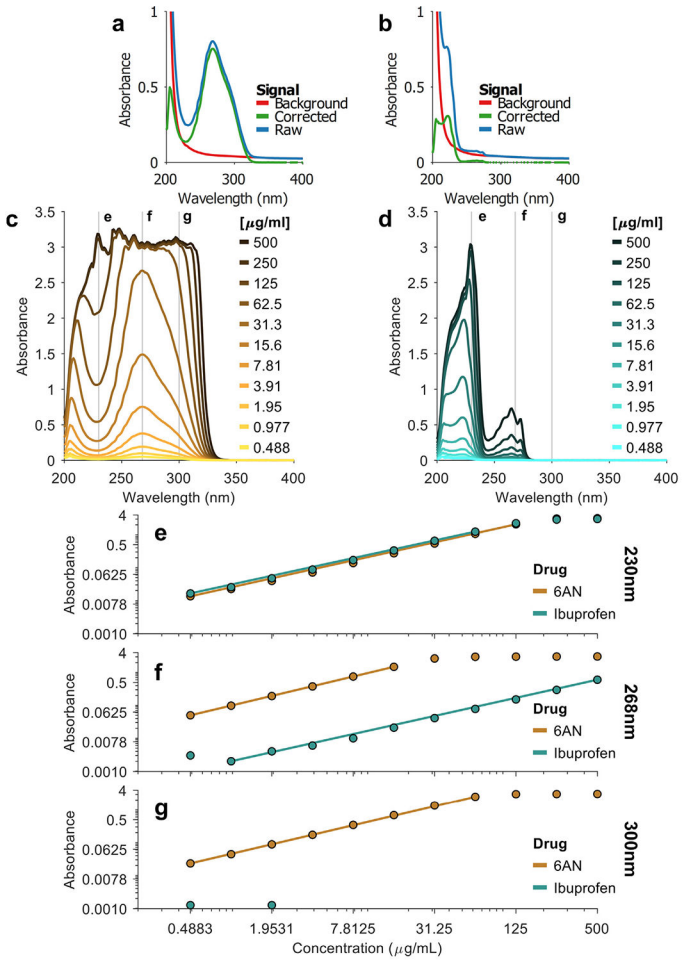

Fig. 1.

A visualization of the method used to identify the linear relationship between drug concentration and absorbance. Panels (a) and (b) are representative spectra of 6AN and Ibuprofen, respectively, dissolved in PBS. The blue line is the signal detected by the UV–Vis spectrometer (Raw), the red line is the signal from PBS with no drug (Background), and green is the difference between the red and blue lines (Corrected). (c) UV–Vis spectra of a 6AN serial dilution with background subtracted, and (d) UV–Vis spectra of Ibuprofen serial dilution with background subtracted. Panels (e–g) are absorbance values for each drug at a single wavelength and demonstrate the correlation between concentration and absorbance. For each plot in (e–g), the points are the absorbance values read by the UV–Vis spectrometer and lines represent the range of values that the algorithm detected to be linearly correlated.

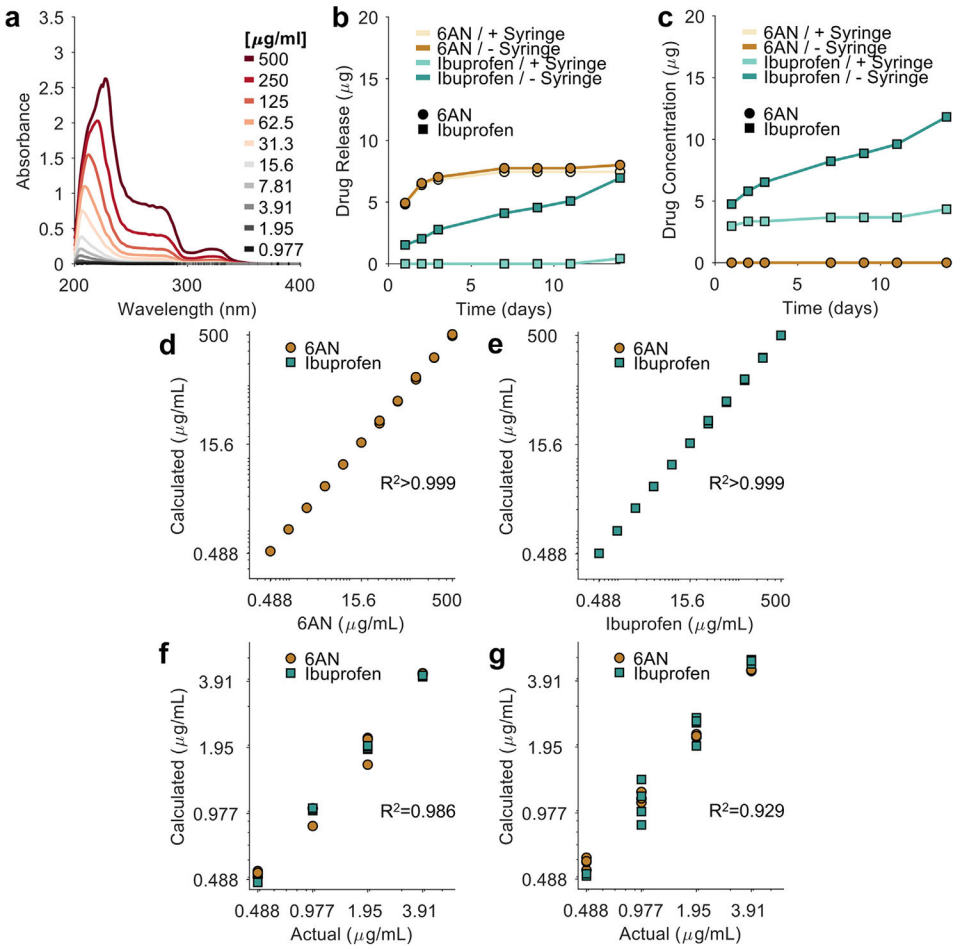

Fig. 2.

Validation of the drug detection method developed in this paper. (a) A serial dilution of 70% ethanol solution exposed to a syringe for 7 days, revealing unknown components in the BD syringes used for electrospinning. The concentrations for the syringe components were unknown, so concentration values in (a) were assigned to match the range of concentrations for Ibuprofen and 6AN. (b) Electrospun fibers containing only 6AN and (c) electrospun fibers containing only Ibuprofen. In (b) and (c), +Syringe is calculation of drug release when syringe components were added to the model, and −Syringe is calculation of drug release without accounting for syringe components. (d) Calculation of the quantity of 6AN and Ibuprofen quantities in the 6AN standard curve (n = 3) when syringe components were included in the model, and only 6AN was detected in the standard curve (as expected). (e) Calculation of 6AN and Ibuprofen quantities in the Ibuprofen standard curve (n = 3) when syringe components were included into the model (only Ibuprofen was detected). (f) All possible combinations of the lowest concentrations were mixed together, and the UV–Vis spectra were used to calculate the amount of drug in each mixture (n = 4). (g) The same mixtures used in f, except syringe components were added to the mixture to determine how the syringe components might impact quantification of each drug (n = 4). For panels d-g, all data points are plotted and thus no error bars are included. The n-values indicate the number

of points per x-axis position. Note that in (d) and (e), all three points at most x-axis locations appear to perfectly overlap.

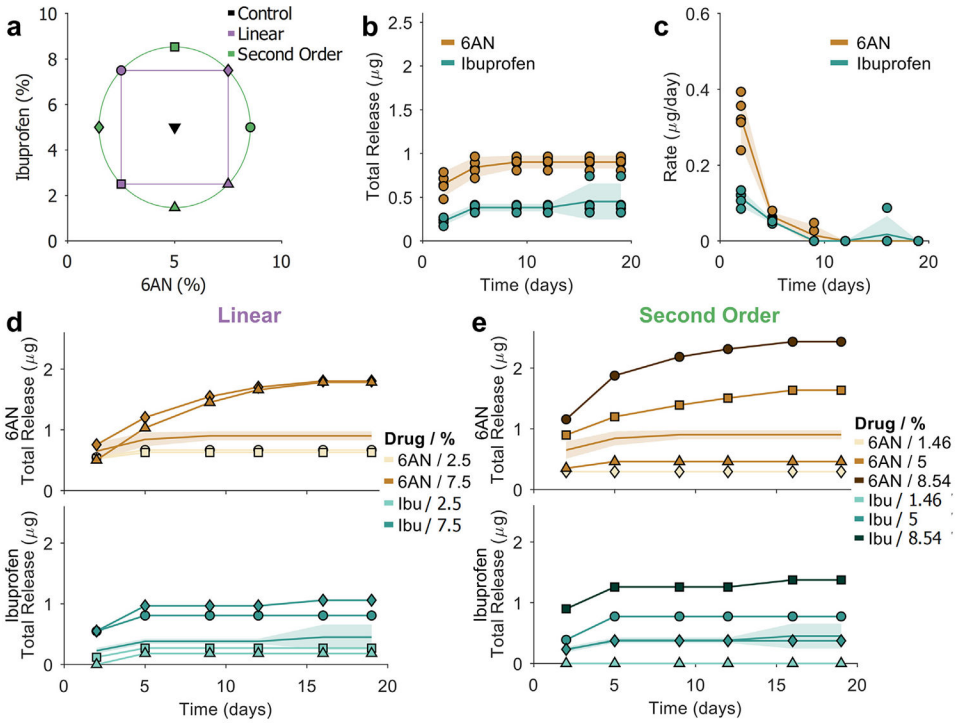

Fig. 3.

Analysis of electrospun fiber diameter and number of fibers/mm. (a) Representative SEM image of electrospun fibers from a control sample (5% each of 6AN and ibuprofen). (b) A histogram of electrospun fiber diameters and a negative binomial distribution fit (black line). (c) A graph of mean fiber diameter for each group, where error bars represent the standard deviation. (d) A graph of the number of fibers per mm of sample for each sample, where error bars represent the standard deviation. Below (c) and (d) is a table showing the amount of each drug and total drug for each sample. Samples are arranged in increasing total drug concentration. Representative images of all 14 groups are available in the Supplemental Figure.

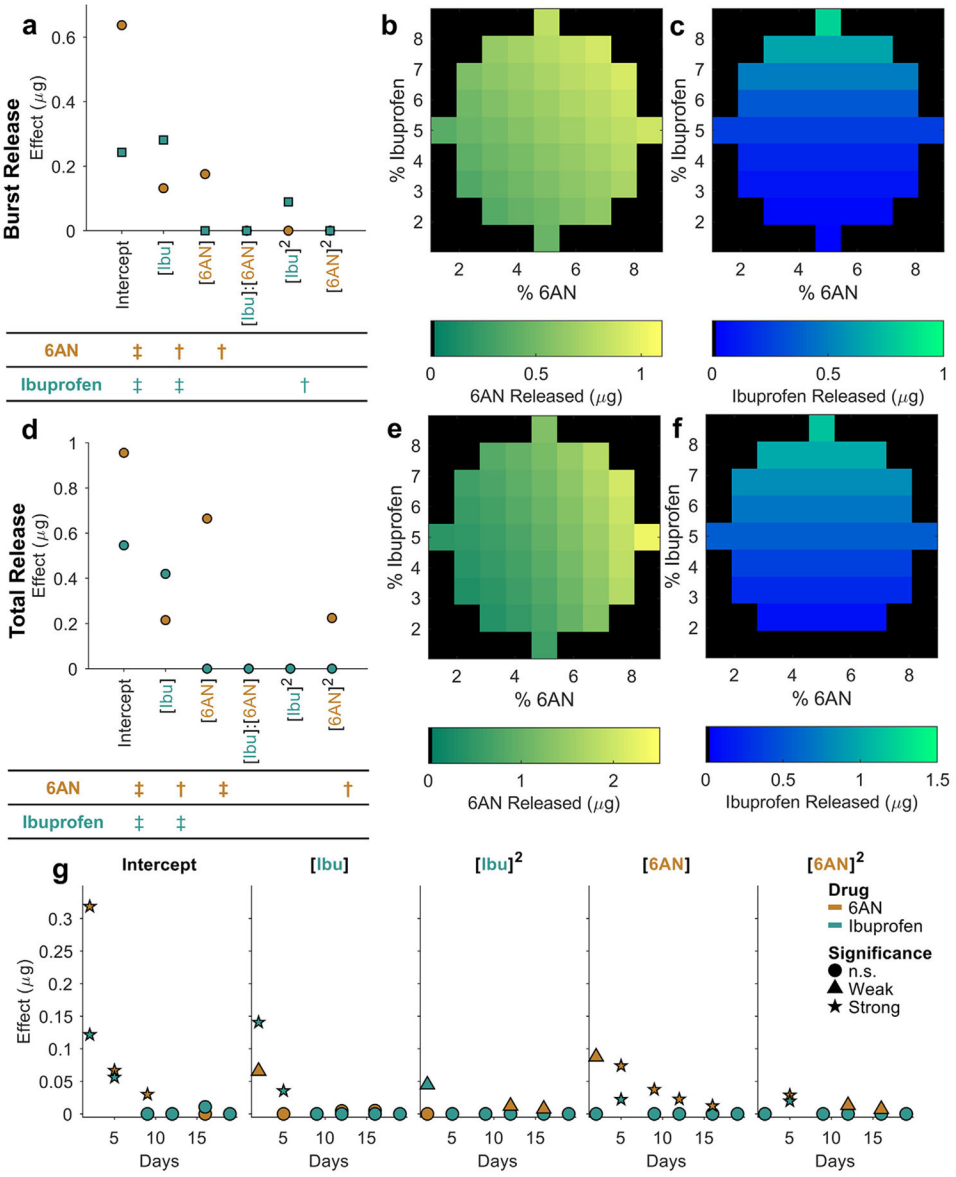

Fig. 4.

Drug release from 13 electrospun fiber scaffolds that contained different amounts of 6AN and Ibuprofen. (a) A visual representation of the experimental space used in this study, where % 6AN and % Ibuprofen refer to the ratio of drug weight to polymer weight. (b) A cumulative release plot of the control groups (n = 5) that simultaneously release 6AN (orange) and Ibuprofen (green), where the solid line represents the mean and the shaded region represents the 95% confidence interval. (c) A plot of release rate of the control groups. (d) Cumulative release plot of the “Linear Effects” groups from panel A. (e) Cumulative release plot of the “Second Order Effects” from panel A. For panels d-e, the top panel is 6AN release (orange) and the bottom panel is Ibuprofen (green), where points that have a matching symbol between the top and bottom panel is the amount of drug released from the same fiber sample. For example, in panel e the circle points in the top panel and the circle points in the bottom panel show the release of 6AN and Ibuprofen (respectively) from

the same fiber sample. The line and shaded region in panels d-e is the mean value of control groups and the 95% confidence interval.

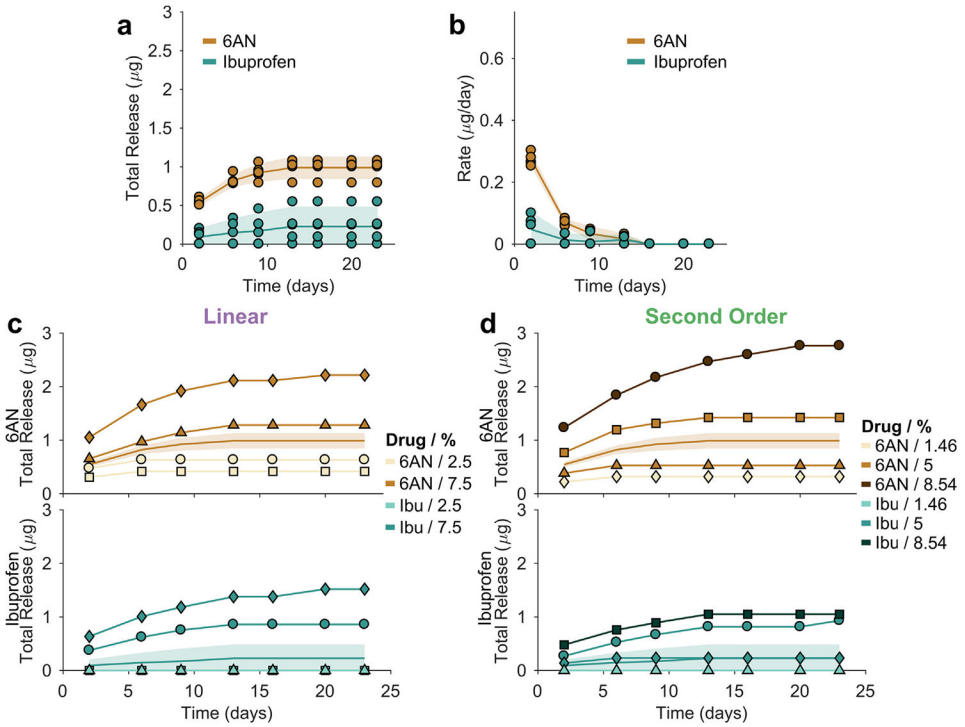

Fig. 5.

An analysis of the models generated from the drug release data. The top row of panels is the "Burst Release" models generated from the drug release data for the first time point (2 days), where (a) is a graph of the best fit model coefficients, (b) is the model surface of 6AN release and (c) is the model surface of Ibuprofen release with respect to 6AN and Ibuprofen loaded into electrospun fibers. The second row of panels is the "Total Release" models generated from the total amount of drug released for each fiber sample, where (d) is a graph of the best fit model coefficients, (e) is the model surface of total 6AN released, (f) is the model surface of total Ibuprofen release. A model was constructed to predict the release rate for each time point. For the graphs in a and d, the color of the point in the graph indicates the drug that is affected by the given variable. For example, in the orange points above Intercept, [6AN], and [Ibu], indicating that both 6AN and Ibuprofen have a linear relationship to 6AN release from the fibers. Symbols below the graph indicate weak significance (†, $p < 0.05$) and strong significance (‡, $p < 0.001$).

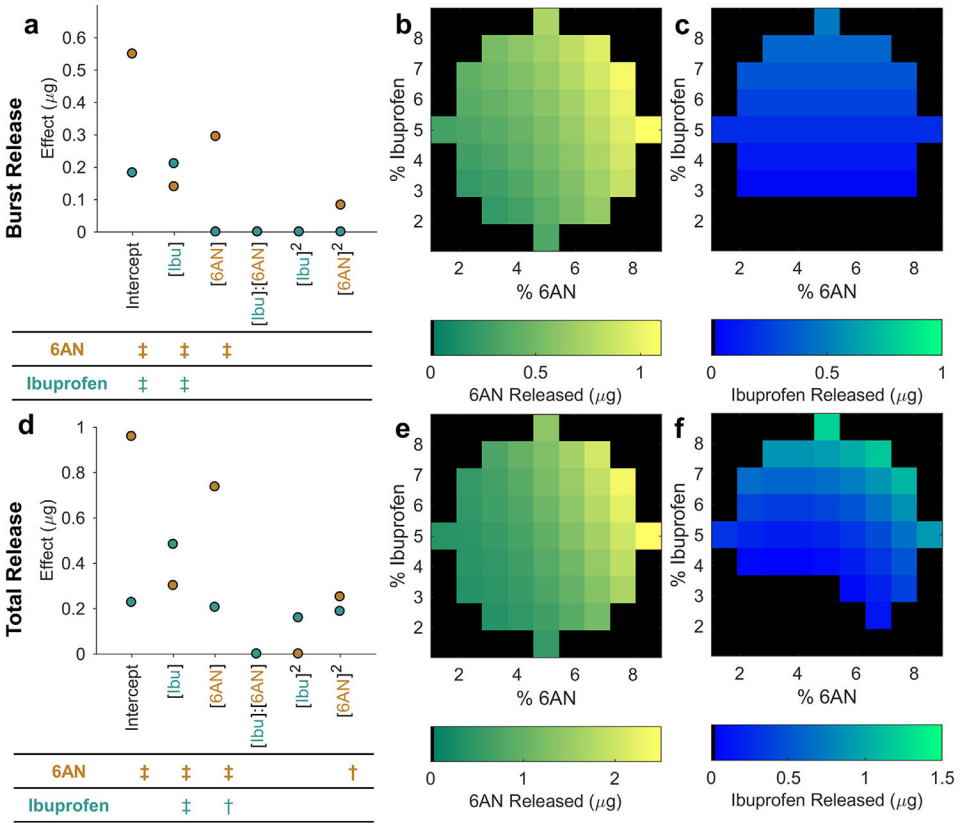

Fig. 6.

Electrospun fibers containing both 6AN and Ibuprofen were aged for one month, then placed in a 37 °C incubator for 4 h without PBS prior to evaluating for drug release. (a) A cumulative release plot of the control groups (n = 5) that simultaneously release 6AN (orange) and Ibuprofen (green), where the solid line represents the mean and the shaded region represents the 95% confidence interval. (b) A plot of release rate of the control groups. (c) Cumulative release plot of the “Linear Effects” groups from Fig. 3a and (d) cumulative release plot of second order groups.

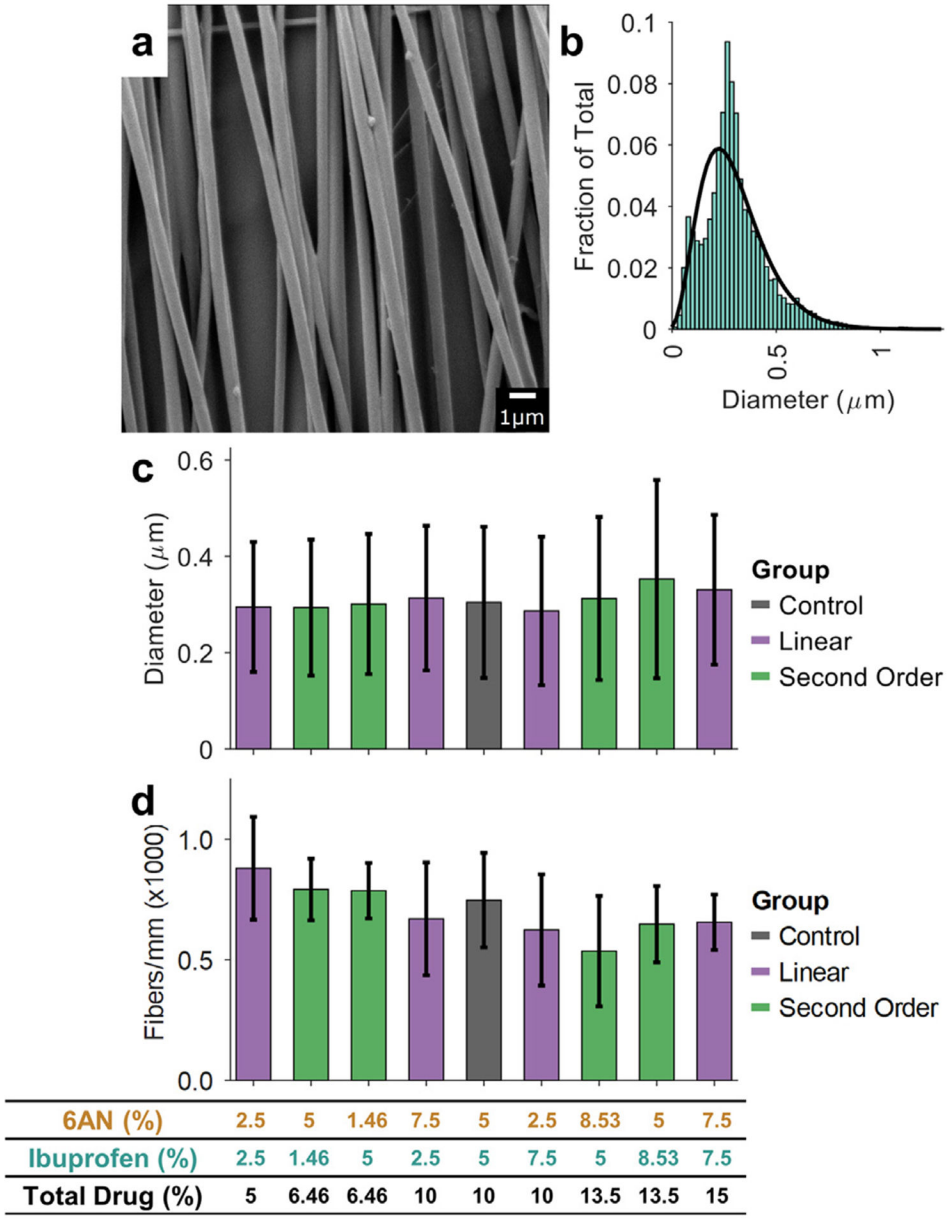

6AN (%)	2.5	5	1.46	7.5	5	2.5	8.53	5	7.5
Ibuprofen (%)	2.5	1.46	5	2.5	5	7.5	5	8.53	7.5
Total Drug (%)	5	6.46	6.46	10	10	10	13.5	13.5	15

Fig. 7.

An analysis of the models generated from the drug release data for fibers that were aged for 1 month and annealed at 37C for four hours. The top row of panels is the “Burst Release” models generated from the drug release data for the first time point (2 days), where (a) is a plot of the model coefficients, (b) and (c) is the 6AN and Ibuprofen (respectively) released with respect to the amount of 6AN and Ibuprofen in each sample. The second row of panels is the “Total Release” models generated from the total amount of drug released for each fiber sample, where (d) is a plot of the model coefficients and (e) and (f) are 6AN and Ibuprofen (respectively) released. Symbols below the plots in (a) and (d) indicate weak significance (†, $p < 0.05$) and strong significance (‡, $p < 0.001$).

Table 1

A list of drug loading concentrations for each electrospun fiber sample. All samples contained the same amount of PLLA and HFP in the electrospinning solution but varied the content of 6AN and Ibuprofen loading as listed here. Percentages in this table are calculated by weight of drug relative to weight PLLA.

	Sample	% 6AN	% Ibuprofen
Linear	1	5	5
	2	5	5
	3	2.5	7.5
	4	5	5
	5	2.5	2.5
	6	7.5	7.5
	7	7.5	2.5
Second Order	8	8.53	5
	9	5	5
	10	5	5
	11	5	8.53
	12	1.46	5
	13	5	5
	14	5	1.46